Journal of Hazardous Materials 161 (2009) 81–87

Contents lists available at ScienceDirect

Journal of Hazardous Materials

journal homepage: www.elsevier.com/locate/jhazmat

Adsorption of methyl *tert*-butyl ether (MTBE) from aqueous solution by porous polymeric adsorbents

Biyan Ji, Fei Shao, Guanjiu Hu, Shourong Zheng, Qingmei Zhang, Zhaoyi Xu *

State Key Laboratory of Pollution Control and Resource Reuse, School of the Environment, Nanjing University, Nanjing 210093, China

ARTICLE INFO

Article history:
Received 10 September 2007
Received in revised form 12 March 2008
Accepted 13 March 2008
Available online 20 March 2008

Keywords:
Postcrosslinked polymeric adsorbent
Postcrosslinking
Methyl *tert*-butyl ether
Adsorption

ABSTRACT

MTBE has emerged as an important water pollutant because of its high mobility, persistence, and toxicity. In this study, a postcrosslinked polymeric adsorbent was prepared by postcrosslinking of a commercial chloromethylated polymer, and a nonpolar porous polymer with comparable surface area and micropore volume to the postcrosslinked polymer was prepared by suspended polymerization. The postcrosslinked polymer, nonpolar porous polymer and chloromethylated polymer were characterized by N_2 adsorption, FTIR and XPS analysis. Results showed that postcrosslinking reaction led to the generation of a microporous postcrosslinked polymer with BET surface area 782 $m^2 g^{-1}$, average pore width 3.0 nm and micropore volume 0.33 $cm^3 g^{-1}$. FTIR and XPS analysis indicated the formation of surface oxygen-containing groups on the postcrosslinked polymer. The three polymers were used as adsorbents to remove aqueous methyl *tert*-butyl ether (MTBE). Adsorption of MTBE over the postcrosslinked polymeric adsorbent was found to follow the linear adsorption isotherm, whereas MTBE adsorption onto the nonpolar porous polymer and chloromethylated polymer followed Langmuir adsorption model. Comparison of adsorption capacities of the postcrosslinked polymer, chloromethylated polymer and nonpolar porous polymer revealed that the adsorption of MTBE from aqueous solution is dependent on both pore structure and surface chemistry of polymeric adsorbents, and the high adsorption efficiency of the postcrosslinked polymer towards MTBE is attributed to its high surface area, large micropore volume and moderate hydrophility. The process of MTBE adsorption onto the adsorbents can be well described by pseudo-second-order kinetics, and the rate of adsorption decreased at higher MTBE initial concentration.

1. Introduction

Methyl *tert*-butyl ether (MTBE) is extensively used as a gasoline additive to increase the octane rating and promote more complete combustion. In recent years, however, the large-scale use of MTBE has led to the widespread contamination of groundwater. Growing concern has been focused on MTBE contamination control since the U.S. Environmental Protection Agency (USEPA) classified MTBE as a possible human carcinogen [1–4]. Nevertheless, MTBE's high water solubility, low Henry's Law constant and resistance to biodegradation complicate its removal from water by conventional treatment techniques [5,6].

Adsorption treatment using porous materials such as activated carbon [7–12], zeolites [7,13,14] and synthetic resins [8,14–19] has been adopted to remove aqueous MTBE. A large amount of adsorption isotherms as well as breakthrough curves [11,12,15,17] were compiled and used to characterize the adsorption properties. Among the potential adsorbents for the abatement of aqueous MTBE, synthetic resin adsorbents with high surface area and tunable pore structure have proved to be the promising candidates [20]. Synthetic carbonaceous resins Ambersorb 563 and 572 were found to have adsorption capacities three to five times greater than activated carbon Filtrasorb 400 at an MTBE equilibrium concentration of 1 mg/l [8]. Shih et al. [17] concluded that Ambersorb 563 was a superior adsorbent for the removal of MTBE from drinking water in terms of adsorbent usage rate, integrated column capacity and the cost. Synthetic polymeric resins Amberlite XAD-4, XAD-7 and Optipore L493 were also found to be effective for the adsorption of aqueous MTBE [15,18,19].

Polymeric resin adsorbents are usually classified into three categories: gel-type, macroporous and postcrosslinked [21]. Gel-type resins with nonporous structure and low surface area are seldom used as the adsorbents for organic solutes. Macroporous resins are capable of effectively adsorbing organic pollutants, due to their porous polymeric matrix. For small organic molecules such as MTBE, however, adsorption generally occurs in the micropores of the resins through van der Waals forces, dipole–dipole interactions, and/or hydrogen bonding [22,23]. It is noteworthy that the pore structure as well as the micropore volume of polymeric adsorbents can be finely tuned by postcrosslinking using chloromethylated

* Corresponding author. Tel.: +86 25 83595831; fax: +86 25 83707304.
E-mail address: zhaoyixu@nju.edu.cn (Z. Xu).

0304-3894/$ – see front matter © 2008 Elsevier B.V. All rights reserved.
doi:10.1016/j.jhazmat.2008.03.052

polymer as starting material via Friedel–Crafts reaction [21,24–26]. Furthermore, the resulting postcrosslinked polymer displays excellent adsorption properties towards both polar and nonpolar organic compounds owning to the large specific surface area and abundant micropore volume [24,27–30]. In the light of previous studies, we speculate that aqueous MTBE can be effectively adsorbed onto postcrosslinked polymer with abundant micropores. To our best knowledge, however, the adsorption behaviors of MTBE from aqueous solution onto postcrosslinked polymer sorbents have rarely been reported in the literature, and the effects of pore structure and surface characteristics of porous polymeric adsorbents on MTBE adsorption remain unclear so far.

In the present study, postcrosslinked polymeric adsorbent was prepared by postcrosslinking of a chloromethylated polymer and adsorption of MTBE from aqueous solution onto the adsorbent was investigated. This study aimed at the characterization of the polymeric adsorbents, determination of the adsorption isotherms and kinetics, and the comparison of adsorption properties of different polymeric adsorbents to elucidate the adsorption mechanism and evaluate the effects of pore structure and surface chemistry of polymeric adsorbents on the adsorption of MTBE.

2. Experimental

2.1. Materials

Commercial coconut shell-based activated carbon Huajing GAC was obtained from Chengde Huajing Activated Carbon Company, China. Amberlite XAD-4 resin was obtained from Rohm & Haas Company, US.

2.2. Preparation of polymeric adsorbents

2.2.1. Preparation of nonpolar porous polymer

Nonpolar porous polymer was prepared by the polymerization of divinylbenzene (the monomer) with gelatin as the diluent, toluene as the porogen and benzoyl peroxide (BPO) as the initiator. The polymerization reaction was carried out in a 500-ml four-necked, round-bottomed flask fitted with mechanical stirrer. Gelatin and distilled water were added to the flask to form a 0.5% (w/w) aqueous solution. An organic phase was prepared by mixing the monomer, the porogen and the initiator. The concentration of initiator was 1% by weight of the monomer, and the ratio of porogen to monomer was 2:1 (v/v). For the polymerization reaction, 120 ml of the organic phase was slowly added to 250 ml of the previously prepared gelatin aqueous solution under stirring at 45 °C. The mixture was first slowly heated to 75 °C and held at this temperature for 2 h, then heated to 85 °C and kept for 4 h and finally heated to 95 °C and held for 3 h. The resulting polymer beads were collected by filtration, followed by washing with hot water and extracting with acetone in a Soxhlet apparatus for 12 h before dried at 80 °C for 8 h.

2.2.2. Preparation of postcrosslinked polymer

Commercial chloromethylated polymer (Chemical Plant of Nankai University, China) with chlorine content of 19.5% was used as the starting material for the preparation of postcrosslinked polymer. Typically, 10 g of the chloromethylated polymer was swollen overnight in 60 ml of nitrobenzene. 1 g zinc chloride was added to the suspension of polymer beads under stirring. The mixture was slowly heated to 110 °C and held at this temperature for 12 h. Afterwards, the resulting polymer beads were recovered by filtration, washed with ethanol and distilled water, and extracted with ethanol in a Soxhlet apparatus for 8 h. The polymer beads were washed with 2 mol/l hydrochloric acid on a magnetic stirrer, and finally dried in an oven for 8 h at 60 °C.

2.3. Characterization of polymeric adsorbents

The Brunauer–Emmett–Teller (BET) surface areas and pore size distributions of the polymeric adsorbents were determined by N_2 adsorption on a Micrometrics ASAP 2010 automatic analyser at −196 °C (77 K). IR Spectra of the polymers were recorded with Nicolet Nexus 870 Spectrometer. X-ray photoelectron spectrometer (VG ESCALAB MK-II) with Mg Kα as X-ray source at a pressure of 10^{-8} mbar was used to analyze the surface properties of polymeric adsorbents. All spectra were obtained using an anode power of 260 W (13 kV, 20 mA) at a pass energy of 20 eV.

2.4. Adsorption isotherms

Adsorption isotherms of MTBE onto commercial chloromethylated polymer, nonpolar porous polymer, and postcrosslinked polymer were determined by batch tests. Carefully weighed amounts of adsorbents were introduced into 50-ml glass tubes containing 50 ml of MTBE aqueous solution with known initial concentrations. The tubes were Teflon sealed and placed in a constant temperature incubating shaker, in which adsorption was allowed to last 48 h at 25 °C to reach the adsorption equilibrium. Samples were then taken from the solution for MTBE concentration measurement using an Agilent 6890 gas chromatograph with purge & trap Tekmar Dohrmann 3100 Sample Concentrator. The adsorption amount of MTBE in the sample was calculated according to the following equation:

$$q_e = \frac{(C_0 - C_e)V}{M} \quad (1)$$

where q_e is the equilibrium adsorption amount (mg g^{-1}), C_0 is the initial concentration of MTBE solution (mg l^{-1}), C_e is the equilibrium concentration of MTBE (mg l^{-1}), V is the volume of MTBE solution (l), and M is the mass of polymeric adsorbent (g).

2.5. Adsorption kinetics

For the measurement of the time-dependent uptake of MTBE onto different polymeric adsorbents, 0.5 g adsorbent was introduced to a 500-ml flask with glass stopper containing 500 ml MTBE aqueous solution with known concentration. The flask was placed in a constant temperature incubating shaker at 25 °C. Aqueous samples were withdrawn from the flask at different time intervals. The concentration of residual MTBE was determined and the adsorption amount was calculated according to the following equation:

$$q_t = \frac{(C_0 - C_t)V}{M} \quad (2)$$

where q_t is the adsorption amount at time t (mg g^{-1}), C_0 is the initial concentration of MTBE solution (mg l^{-1}), C_t (mg l^{-1}) is MTBE concentration at time t, V is the volume of MTBE solution (l), and M is the mass of polymeric adsorbent (g).

3. Results and discussion

3.1. Material characterization

The BET surface areas (S_{BET}), pore volumes, and other structural properties of the adsorbents are listed in Table 1. The pore size distribution of the polymers is illustrated in Fig. 1. The nonpolar porous polymer had a specific surface area of 656.4 m^2 g^{-1}, implying that the polymer consists of a porous network instead of a conventional gel structure. Nyhus et al. [32] reported that polymerization of *meta*-DVB and *para*-DVB with toluene as the porogen resulted in a porous polymer with the specific surface area up to 1000 m^2 g^{-1}. N_2 adsorption analysis results showed that the pore volume of the polymer was 0.94 cm^3 g^{-1}, demonstrating the porosity of this

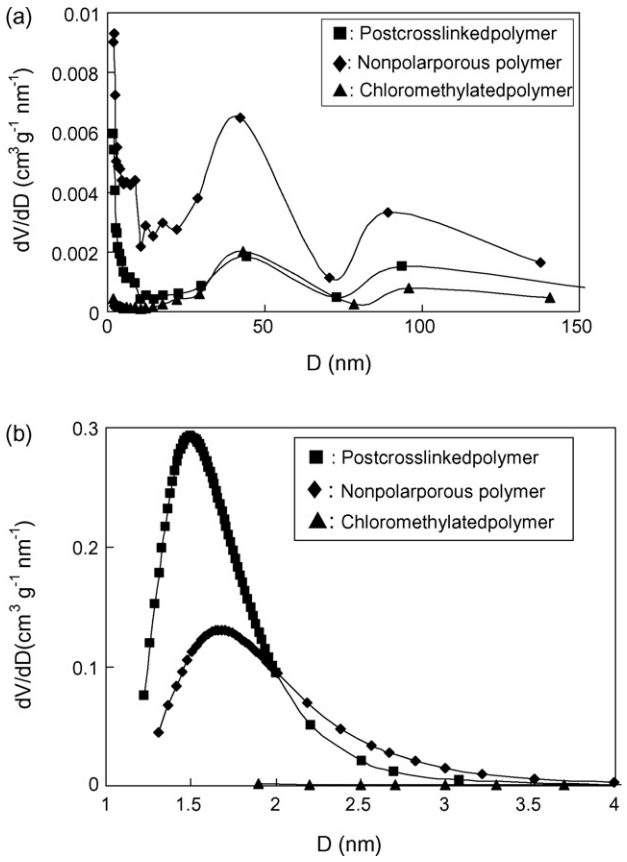

Fig. 1. Pore size distributions of the polymeric adsorbents.

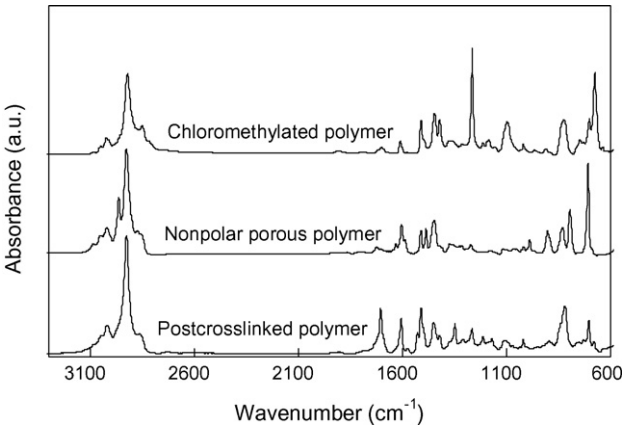

Fig. 2. IR spectra of the polymeric adsorbents.

polymer. Typically, two types of porogens, good solvents and non-solvents, are frequently used in the preparation of porous polymer [24]. Polymers prepared in a good solvent, such as toluene, are usually found to be more microporous. Investigation of the morphology and pore size distribution of poly(*meta*-DVB) and poly(*para*-DVB) prepared in the presence of toluene indicated that the resulting porous polymers were mainly composed of micropores [32]. In the presence of a good solvent the generation of micropores is generally associated with the effective solvating of the growing polymer chains, which consequently delays the precipitation of the polymer. The retarded phase separation leads to an enhanced crosslinking between polymer chains and eventually to an increased microporosity.

The polymer with abundant micropores was also prepared via postcrosslinking of the chloromethylated polymer. The specific surface area of the commercial chloromethylated polymer was determined to be 35.8 $m^2\,g^{-1}$. After postcrosslinking process, the specific surface area increased up to 782.0 $m^2\,g^{-1}$. Jerabek et al. [28] studied postcrosslinking of chloromethylated copolymer and found that polymers with specific surface areas of 940 and 720 $m^2\,g^{-1}$ could be obtained by postcrosslinking process using gel-type chloromethylated polymer and macroreticular chloromethylated polymer as the precursors, respectively. This clearly demonstrates that the surface area of the chloromethylated polymer can be markedly enhanced via the postcrosslinking process.

Postcrosslinking procedure also led to changes in the pore structure of the resulting polymer. N_2 adsorption results showed that the chloromethylated polymer had an average pore width of 16.7 nm and pore volume of 0.30 $cm^3\,g^{-1}$. In contrast, the postcrosslinked polymer was characteristic of an average pore width of 3.0 nm and pore volume of 0.55 $cm^3\,g^{-1}$. The postcrosslinked polymer exhibited a similar pore size distribution to the chloromethylated polymer in pore diameter between 2 and 150 nm. It is worthy to note that the postcrosslinked polymer displayed an extremely sharp and narrow pore size distribution in pore diameter between 1 and 2 nm, in which the maximum dV/dD value was observed at pore diameter of 1.5 nm. In comparison, the chloromethylated polymer gave a very low dV/dD value at pore diameter lower than 2 nm. In parallel, the micropore volume of the postcrosslinked polymer was 0.33 $cm^3\,g^{-1}$, which is markedly higher than that of the chloromethylated polymer (see Table 1). This clearly points out that the postcrosslinked polymer possessed abundant micropores and the increased pore volume and narrowed pore width are mainly attributed to the new generated micropores.

The structural changes in the chloromethylated polymer after postcrosslinking can be followed using IR spectrometer and IR spectra of the polymers are compared in Fig. 2. For the IR spectrum of the chloromethylated polymer, IR bands at 3104, 3060 and 3027 cm^{-1} are characteristic of C–H stretching vibration from aromatic rings. IR bands at 2924 and 2875 cm^{-1} are assigned to the C–H stretching vibration from alkyl groups. IR bands at 1512, 1448, 1423 and 1382 cm^{-1}, characteristic of aromatic C–C and alkyl C–H vibration, were also visible. The aromatic C–H vibrations were evidenced by IR bands at 831, 754 and 704 cm^{-1}. Note that a strong IR band at 675 cm^{-1}, characteristic of C–Cl vibration, was observed. In parallel, a strong IR band at 1265 cm^{-1} characteristic of C–H vibration from chloromethyl groups was also observed, reflecting the presence of benzyl chloride in the polymer. After postcrosslinking, the strength of IR bands at 1265

Table 1
Structural properties of the adsorbents

Sample	BET surface area ($m^2\,g^{-1}$)	Average pore width (nm)	Pore volume ($cm^3\,g^{-1}$)	Micropore volume ($cm^3\,g^{-1}$)
Chloromethylated polymer	35.8	16.7	0.30	–
Nonpolar porous polymer	656.4	6.7	0.94	0.28
Postcrosslinked polymer	782.0	3.0	0.55	0.33
Amberlite XAD-4[a]	750.0	5.0	–	–
Huajing GAC	661.3	1.9	0.32	0.27

[a] From Ref. [31].

Table 2
Compositions of surface elements on the polymeric adsorbents derived from XPS analysis

Sample	C (wt.%)	O (wt.%)	Cl (wt.%)
Chloromethylated polymer	83.9	2.6	13.5
Nonpolar porous polymer	100	0	0
Postcrosslinked polymer	92.3	4.3	3.4

and 675 cm^{-1} markedly reduced, indicative of the decreased content of chloromethyl groups in the postcrosslinked polymer. The decrease in the content of chloromethyl groups can be ascribed to Friedel–Crafts reaction between chloromethyl groups and vicinal aromatic rings. In addition, a strong IR band at 1704 cm^{-1} was observed, reflecting the presence of carbonyl groups in the polymer. Xu et al. [33] studied the postcrosslinking of chloromethylated polymers with nitrobenzene as the solvent and found that at reaction temperature higher than 120 °C benzyl chloride groups could be oxidized into carbonyl groups. Similar results were also obtained by Meng et al. [34].

XPS analysis results are listed in Table 2. The surface chlorine content of the nonpolar porous polymer was not determinable due to the absence of chloric reagent used in the preparation process. Postcrosslinking of the chloromethylated polymer led to a decrease of the surface chlorine content from 13.5 to 3.4 wt.%, indicating that approximate 75% of the surface chlorine was consumed during the postcrosslinking process. Fontanals et al. [26] studied the synthesis of postcrosslinked polymers and observed substantial decrease in chlorine content during the reaction course, which is associated with conversion of the chloromethyl groups into the methylene bridges.

XPS results further showed that the surface oxygen contents of the nonpolar porous polymer, the chloromethylated polymer and the postcrosslinked polymer were 0, 2.6 and 4.3 wt.%, respectively. In fact, surface oxygen with markedly high content was also identified in commercial postcrosslinked polymers Purolite MN-200 and MN-600 [35,36], which is consistent with the observations of Xu et al. [33] and Meng et al. [34]. Note that the surface oxygen content is related to the hydrophilicity of the polymeric resins [26,33–36]. Therefore, the higher surface oxygen content suggests the partial hydrophilicity of the postcrosslinked polymer compared to the hydrophobic nonpolar porous polymer and the chloromethylated polymer.

3.2. Adsorption isotherms

The adsorption isotherms of MTBE over the different adsorbents at 25 °C are compared in Fig. 3. Among the adsorbents investigated, the postcrosslinked polymer has the highest adsorption capacity towards aqueous MTBE. Note that Huajing GAC used in this study had a BET surface area of 661.3 $m^2\,g^{-1}$, whereas commercial activated carbons with surface area more than 800 or even 1000 $m^2\,g^{-1}$ demonstrated much higher adsorption capacity for MTBE [11,12]. Taking the manufacturing costs into consideration, the postcrosslinked polymer is not yet cost competitive relative to activated carbon. Further work is in progress to improve the adsorption capacity of postcrosslinked polymer at reduced cost, and the results of investigation will be reported in the future.

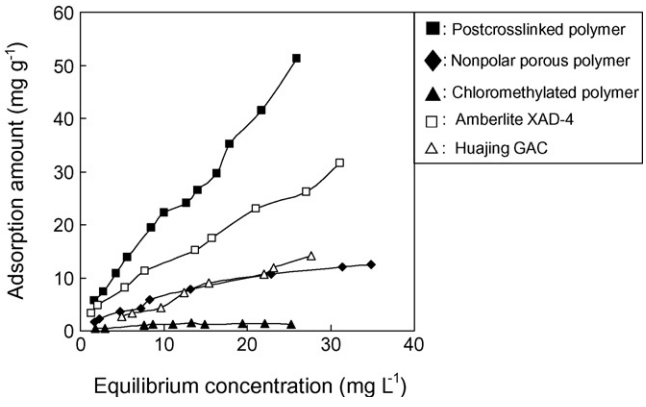

Fig. 3. Adsorption isotherms of MTBE over the polymeric adsorbents at 298 K.

For MTBE adsorption onto the chloromethylated polymer and the nonpolar porous polymer, typical L-type isotherms were observed. In contrast, a linear adsorption isotherm was observed for MTBE adsorption over the postcrosslinked polymer.

To elucidate the mechanism of MTBE adsorption onto the polymeric adsorbents, simulation of the adsorption isotherms was conducted. Simulation results showed that the adsorption isotherms of MTBE over the chloromethylated polymer and nonpolar porous polymer could be well described by Langmuir adsorption model,

$$q_e = \frac{q_\infty b C_e}{1 + bC_e}$$

where q_e is the equilibrium adsorption capacity of polymeric adsorbents (mg g^{-1}), C_e is the equilibrium MTBE concentration in the aqueous solution (mg l^{-1}), q_∞ is the maximum adsorption capacity (mg g^{-1}), and b is the isotherm parameter (l mg^{-1}), respectively.

The adsorption of MTBE over the postcrosslinked polymer followed the linear adsorption isotherm:

$$q_e = K_D C_e$$

where q_e is the equilibrium adsorption capacity (mg g^{-1}), C_e is the equilibrium MTBE concentration (mg l^{-1}), and K_D (l g^{-1}) is the partition coefficient, respectively.

The isotherm parameters obtained are summarized in Table 3. The adsorption behaviors of MTBE onto the postcrosslinked polymer are different from those of the chloromethylated polymer and nonpolar porous polymer. The kinetic diameter of MTBE is reported to be 0.62 nm [37]. Li et al. studied the adsorption of aqueous MTBE onto activated carbon fibers (ACFs) and proposed that the adsorption capacity of ACFs for MTBE was correlated to the pore volume of micropores with pore widths of 0.8–1.1 nm, which was corresponding to 1.3–1.8 times as wide as the kinetic diameter of MTBE molecule [9]. N_2 adsorption results showed that the chloromethylated polymer contained a small BET surface area of 35.8 $m^2\,g^{-1}$ without any micropore volume detected. In addition, the average pore width of the chloromethylated polymer is 16.7 nm, approximately 25 times larger than the kinetic diameter of MTBE. This suggests that the chloromethylated polymer is not an appropriate adsorbent for MTBE, evidenced by the fact that MTBE adsorption capacity was markedly lower compared to the other two polymers. In contrast, the postcrosslinking reaction led to the generation of a micropore-dominant structure as well as significantly increased specific surface area. Note that micropore width of the postcrosslinked polymer is concentrated in the range from 1 to 2 nm. This clearly points out that MTBE molecules can be feasibly adsorbed in the micropores of the postcrosslinked polymer, which is in good agreement with the adsorption data.

The nonpolar porous polymer has the micropore volume of 0.28 $cm^3\,g^{-1}$ and surface area of 656.4 $m^2\,g^{-1}$, which is comparable to the postcrosslinked polymer. Nevertheless, the former showed markedly lower adsorption capability towards MTBE compared to the latter, implying the uptake of aqueous MTBE is not only dominated by the surface area and micropore volumes. In general, MTBE is considered as a hydrophilic compound with high water solu-

Table 3
Isotherm parameters for MTBE adsorption at 298 K

Sample	Model	Parameter			R^2
		q_∞ (mg g^{-1})	b (l mg^{-1})	K_D (l g^{-1})	
Chloromethylated polymer	Langmuir	2.18	0.118	–	0.977
Nonpolar porous polymer	Langmuir	14.8	0.076	–	0.985
Postcrosslinked polymer	Linear	–	–	1.962	0.979

bility due to the high concentration of polar oxygen atom in the molecule. It is a general consensus that the hydrophilic surface is prerequisite for the effective adsorption of hydrophilic adsorbate. Li et al. compared MTBE adsorption onto ACFs with different surface properties and concluded that the ACFs with oxygen and nitrogen content of 2–3 mmol g^{-1} are most effective for the adsorption of hydrophilic MTBE [9]. XPS results showed that surface oxygen content of the postcrosslinked polymer was 4.3 wt.%, corresponding to 2.7 mmol g^{-1}. In contrast, the surface oxygen content of the nonpolar porous polymer was not determinable. Therefore, it can be concluded that the higher MTBE adsorption capability of the postcrosslinked polymer is attributed to its higher surface hydrophilicity compared to the hydrophobic nonpolar porous polymer. This conclusion is further supported by the results of MTBE adsorption over the chloromethylated polymer. For the nonpolar porous polymer and chloromethylated polymer, MTBE adsorption over the adsorbents followed Langmuir adsorption model and the adsorption parameter b in Langmuir adsorption model is characteristic of the affinity of the adsorbate to the adsorption sites on the surface of the adsorbent. The adsorption parameter b of the chloromethylated polymer and nonpolar porous polymer were 0.118 and 0.076, respectively, indicative of the stronger adsorption of MTBE onto the chloromethylated polymer although the adsorption capacity of the chloromethylated polymer is lower than the nonpolar porous polymer. It is noteworthy that the surface oxygen content of the chloromethylated polymer was 2.6 wt.%, higher than that of the nonpolar porous polymer. This also clearly points out that MTBE tends to be adsorbed by more hydrophilic surface.

3.3. Adsorption kinetics of MTBE over polymeric adsorbents

The time courses of MTBE adsorption over polymeric adsorbents at 25 °C are presented in Fig. 4. For the chloromethylated polymer and nonpolar porous polymer, MTBE adsorption was very fast during the initial 60 min and reached the adsorption equilibrium after adsorption for 140 and 240 min, respectively. In contrast, adsorption of MTBE over the postcrosslinked polymer was relatively slow and did not reach equilibrium after adsorption for 1500 min.

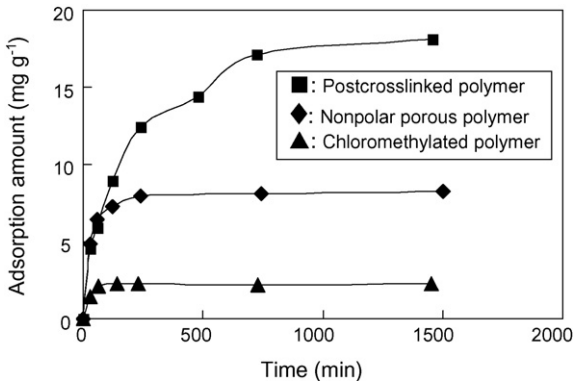

Fig. 4. Adsorption kinetics of MTBE onto the polymeric adsorbents at 298 K.

Among the kinetic models, pseudo-first-order or pseudo-second-order kinetics is the most widely used model to describe the adsorption process [38,39].

The pseudo-first-order kinetics:

$$\log(q_e - q_t) = \log q_e - \frac{k_1}{2.303}t$$

The pseudo-second-order kinetics:

$$\frac{t}{q_t} = \frac{1}{k_2 q_e^2} + \frac{t}{q_e}$$

where q_e is the equilibrium adsorption amount (mg g^{-1}), q_t is the adsorption amount at time t (mg g^{-1}), k_1 is the pseudo-first-order rate constant (min^{-1}) and k_2 is the pseudo-second-order rate constant (g mg^{-1} min^{-1}).

For three polymeric adsorbents, the plot of $\log(q_e - q_t)$ versus t based on pseudo-first-order kinetics and the plot of t/q_t versus t based on pseudo-second-order kinetics are illustrated in Fig. 5. The correlation of pseudo-first-order kinetics (Fig. 5a) did not give a good regression. On the contrary, the good linear plot of t/q_t versus t in Fig. 5b with correlation coefficient (R^2) higher than 0.99 suggests that MTBE adsorption onto the polymeric adsorbents follows the pseudo-second-order kinetic model. The kinetic model parameters are listed in Table 4. For all the three polymeric adsorbents, the q_e values calculated from the slopes of the t/q_t versus t plots were found to be in good agreement with the experimental q_e values, further indicating that the adsorption of aqueous MTBE onto polymeric adsorbents perfectly obey pseudo-second-order kinetics. The adsorption rate constants were calculated to be 4.33×10^{-2}, 6.21×10^{-3} and 3.07×10^{-4} g mg^{-1} min^{-1} for the chloromethylated polymer, nonpolar porous polymer and postcrosslinked polymer, respectively. Note that the average pore widths of the three polymeric adsorbents are 16.7, 6.7 and 3.0 nm, respectively. The lower rate constant of MTBE adsorption onto the postcrosslinked polymer is tentatively attributed to MTBE diffusion into the micropores of the postcrosslinked polymer.

To evaluate the effect of initial concentrations on the adsorption kinetics of MTBE onto the postcrosslinked polymer, the time courses of MTBE adsorption with different initial concentrations are presented in Fig. 6. Fitting results showed that the adsorption of MTBE with different initial concentrations followed pseudo-second-order kinetic model and the adsorption parameters are listed in Table 5. The adsorption rate constants were found to be 3.07×10^{-4}, 2.95×10^{-4} and 1.89×10^{-4} g mg^{-1} min^{-1} at MTBE initial concentrations of 26.5, 47.0 and 85.8 mg l^{-1}, respectively, indicating a decreased adsorption rate at higher initial concentration or MTBE adsorption amount. At low adsorption amounts, MTBE molecules tend to be quickly adsorbed into the open pores of polymeric adsorbents. At high adsorption amounts, however, MTBE molecules have to penetrate into the pores via a longer diffusion length, which eventually results in a decreased adsorption rate at high adsorption amount or initial concentration.

In well-stirred batch adsorption systems the intraparticle diffusion model has been used to describe the adsorption process

Table 4
Pseudo-second-order adsorption rate constants and the calculated and experimental q_e values for adsorption of MTBE on the polymeric adsorbents

Sample	q_e (experimental) (mg g^{-1})	k_2 (g mg^{-1} min^{-1})	q_e (calculated) (mg g^{-1})	R^2
Chloromethylated polymer	2.28	4.33×10^{-2}	2.28	0.999
Nonpolar porous polymer	8.28	6.21×10^{-3}	8.38	1
Postcrosslinked polymer	19.62	3.07×10^{-4}	20.66	0.998

Table 5
Kinetic model parameters for the adsorption of MTBE at different initial concentrations on the postcrosslinked polymer

C_0 (mg l^{-1})	q_e (experimental) (mg g^{-1})	k_2 (g mg^{-1} min^{-1})	q_e (calculated) (mg g^{-1})	R^2
26.5	19.62	3.07×10^{-4}	20.66	0.998
47.0	31.81	2.95×10^{-4}	32.68	0.999
85.8	54.74	1.89×10^{-4}	55.87	0.999

occurring on porous adsorbent [40,41]:

$$q_t = k_i t^{1/2} + x_i$$

where q_t is the adsorption amount at time t (mg g^{-1}), k_i is rate constant for the intraparticle diffusion (mg g^{-1} min$^{-1/2}$) and x_i is the intercept of the line (mg g^{-1}) which is proportional to the boundary layer thickness.

Fig. 7 presents the plots of q_t versus $t^{1/2}$ for adsorption of MTBE onto the postcrosslinked polymer at different initial concentrations and the parameters are listed in Table 6. The results showed that the intraparticle diffusion model well described MTBE adsorption processes, and the values of k_i increased with increasing initial concentrations of MTBE. In addition, three consecutive steps were observed on each plot, with the first steep linear step corresponding to fast uptake of MTBE [42]. It is noteworthy that each line in the first stage passes through the origin, indicating that MTBE adsorption in the initial stage is dominated by the intraparticle diffusion instead of film diffusion process. This can be attributed to the diffusion of MTBE molecules into the micropores of the postcrosslinked polymer, which is relatively slow due to the narrow pore width of the micropores. MTBE adsorption slows down in later stages, reflecting the consecutive diffusion of MTBE molecules into the micropores with narrower pore widths in the postcrosslinked polymer.

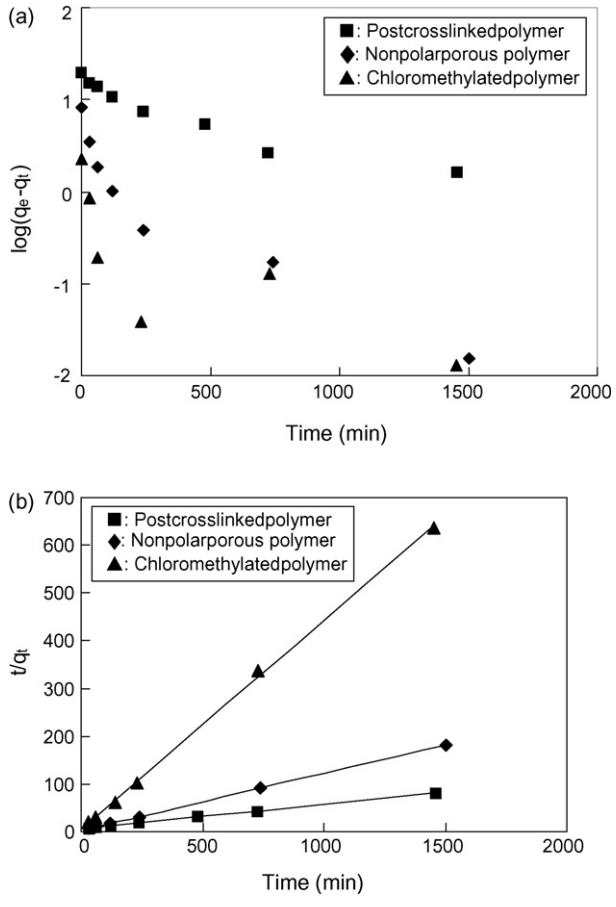

Fig. 5. Simulation of MTBE adsorption onto the polymeric adsorbents using (a) pseudo-first-order kinetics and (b) pseudo-second-order kinetics.

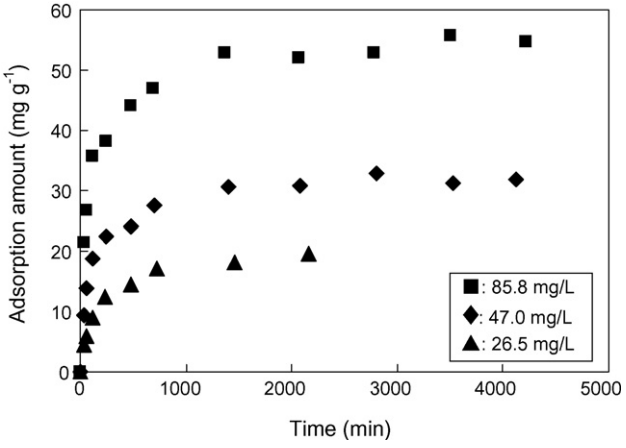

Fig. 6. Adsorption kinetics of MTBE onto the postcrosslinked polymer at different initial concentrations.

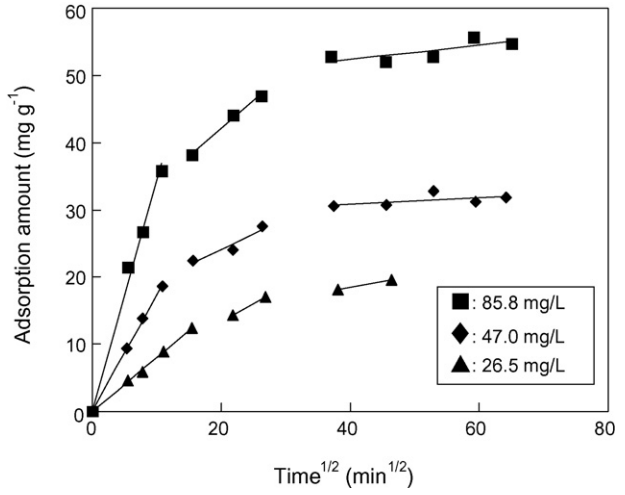

Fig. 7. Plots of q_t versus $t^{1/2}$ for adsorption of MTBE on the postcrosslinked polymer at different initial concentrations.

Table 6
Intraparticle diffusion constants for adsorption of MTBE on the postcrosslinked polymer at different initial concentrations

C_0 (mg l^{-1})	k_i (mg g^{-1} min$^{-1/2}$)	R^2
26.5	0.80	0.999
47.0	1.73	0.999
85.8	3.43	0.990

4. Conclusions

In this study, the postcrosslinked polymer and nonpolar porous polymer were prepared and MTBE adsorption onto the nonpolar porous, chloromethylated and postcrosslinked polymeric adsorbents was investigated. The postcrosslinking reaction of the chloromethylated polymer results in increased surface area, abundant micropores and partial surface hydrophilicity in the postcrosslinked polymer, which leads to the markedly higher adsorption capacity for aqueous MTBE compared to nonpolar porous and chloromethylated polymers. Based on the correlation of the structural properties to the adsorption behaviors of the polymers, MTBE adsorption is concluded to be dominated by the pore structure and surface chemistry of the polymeric adsorbents. The abundant micropores as well as moderate surface hydrophilicity are favorable for MTBE adsorption onto the polymer. For adsorption kinetics, MTBE adsorption onto the polymers follows the pseudo-second-order model. In addition, MTBE diffusion into the postcrosslinked polymer is controlled by the intraparticle diffusion due to the preferential adsorption of MTBE in the micropores.

Acknowledgements

The authors acknowledge support from the National Natural Science Foundation of China (Grant no. 40402022, 20677026), Natural Science Foundation of Jiangsu Province, China (Grant no. BK2005417), National Scientific and Technical Supporting Program of China (Grant no. 2006BAC02A15) and Hi-Tech Research and Development Program (863 Program) of China (Grant no. 2006AA06Z383). We also thank Modern Analytical Center, Nanjing University for the characterization of materials.

References

[1] U.S. Environmental Protection Agency, Oxygenates in water: critical information and research needs, EPA/600/R-98/048, 1998.
[2] U.S. Environmental Protection Agency, Achieving clean air and clean water. The report of the blue ribbon panel on oxygenates in gasoline, EPA 420-R-99-021, 1999.
[3] F.E. Ahmed, Toxicology and human health effects following exposure to oxygenated or reformulated gasoline, Toxicol. Lett. 123 (2001) 89–113.
[4] R. Johnson, J. Pankow, D. Bender, C. Price, J. Zogorski, MTBE: to what extent will past releases contaminate community water supply wells, Environ. Sci. Technol. 34 (2000) 210A–217A.
[5] R.W. Gullick, M.W. LeChevallier, Occurrence of MTBE in drinking water sources, J. AWWA 92 (2000) 100–113.
[6] N.Y. Fortin, M. Morales, Y. Nakagawa, D.D. Focht, M.A. Deshusses, Methyl *tert*-butyl ether (MTBE) degradation by a microbial consortium, Environ. Microbiol. 3 (2001) 407–416.
[7] M.A. Anderson, Removal of MTBE and other organic contaminants from water by sorption to high silica zeolites, Environ. Sci. Technol. 34 (2000) 725–727.
[8] S.W. Davis, S.E. Powers, Alternative sorbents for removing MTBE from gasoline-contaminated ground water, J. Environ. Eng. 126 (2000) 354–360.
[9] L. Li, P.A. Quinlivan, D.R.U. Knappe, Effects of activated carbon surface chemistry and pore structure on the adsorption of organic contaminants from aqueous solution, Carbon 40 (2002) 2085–2100.
[10] L. Yu, C. Adams, D. Ludlow, Adsorption isotherms for methyl *tert*-butyl ether and other fuel oxygenates on two bituminous-coal activated carbons, J. Environ. Eng. 131 (2005) 983–987.
[11] W.C. Ying, W. Zhang, Q.G. Chang, W.X. Jiang, G.H. Li, Improved methods for carbon adsorption studies for water and wastewater treatment, Environ. Prog. 25 (2006) 110–120.
[12] W. Zhang, Q.G. Chang, W.D. Liu, B.J. Li, W.X. Jiang, L.J. Fu, W.C. Ying, Selecting activated carbon for water and wastewater treatability studies, Environ. Prog. 26 (2007) 289–298.
[13] S.G. Li, V.A. Tuan, R.D. Noble, J.L. Falconer, MTBE adsorption on all-silica beta zeolite, Environ. Sci. Technol. 37 (2003) 4007–4010.
[14] H.W. Hung, T.F. Lin, Adsorption of MTBE from contaminated water by carbonaceous resins and mordenite zeolite, J. Hazard. Mater. B 135 (2006) 210–217.
[15] M.C. Annesini, F. Gironi, B. Monticelli, Removal of oxygenated pollutants from wastewater by polymeric resins: data on adsorption equilibrium and kinetics in fixed beds, Water Res. 34 (2000) 2989–2996.
[16] S.H. Lin, C.S. Wang, C.H. Chang, Removal of methyl *tert*-butyl ether from contaminated water by macroreticular resin, Ind. Eng. Chem. Res. 41 (2002) 4116–4121.
[17] T. Shih, M. Wangpaichitr, M. Suffet, Performance and cost evaluations of synthetic resin technology for the removal of methyl *tert*-butyl ether from drinking water, J. Environ. Eng. 131 (2005) 450–460.
[18] E. Bi, S.B. Haderlein, T.C. Schmidt, Sorption of methyl *tert*-butyl ether (MTBE) and *tert*-butyl alcohol (TBA) to synthetic resins, Water Res. 39 (2005) 4164–4176.
[19] A. Flores, A. Stocking, M. Kavanaugh, Synthetic resin sorbents, in: G. Melin (Ed.), Treatment Technologies for Removal of Methyl Tertiary Butyl Ether (MTBE) from Drinking Water: Air Stripping, Advanced Oxidation Processes, Granular Activated Carbon, Synthetic Resin Sorbents, National Water Research Institute, California, 2000, pp. 261–333.
[20] Z. Xu, Q. Zhang, H.H.P. Fang, Applications of porous resin sorbents in industrial wastewater treatment and resource recovery, Crit. Rev. Environ. Sci. Technol. 33 (2003) 363–389.
[21] M.P. Tsyurupa, L.A. Maslova, A.I. Andreeva, T.A. Mrachkovskaya, V.A. Davankov, Sorption of organic compounds from aqueous media by hypercrosslinked polystyrene sorbents 'Styosorb', React. Polym. 25 (1995) 69–78.
[22] Rohm and Haas Company, Ambersorb carbonaceous adsorbents: specialty purifications, 1992.
[23] G.R. Parker, Optimum isotherm equation and thermodynamic interpretation for aqueous 1,1,2-trichloroethene adsorption isotherms on three adsorbents, Adsorption 1 (1995) 113–132.
[24] M.P. Tsyurupa, V.A. Davankov, Porous structure of hypercrosslinked polystyrene: state-of-the-art mini-review, React. Funct. Polym. 66 (2006) 768–779.
[25] P. Veverka, K. Jerabek, Mechanism of hypercrosslinking of chloromethylated styrene-divinylbenzene copolymers, React. Funct. Polym. 41 (1999) 21–25.
[26] N. Fontanals, J. Cortes, M. Galia, R.M. Marce, P.A.G. Cormack, F. Borrull, D.C. Sherrington, Synthesis of Davankov-type hypercrosslinked resins using different isomer compositions of vinylbenzyl chloride monomer, and application in the solid-phase extraction of polar compounds, J. Polym. Sci. Polym. Chem. 43 (2005) 1718–1728.
[27] V.A. Davankov, M.P. Tsyurupa, Structure and properties of hypercrosslinked polystyrene-the first representative of a new class of polymer networks, React. Polym. 13 (1990) 27–42.
[28] K. Jerabek, L. Hankova, Z. Prokop, Post-crosslinked polymer adsorbents and their properties for separation of furfural from aqueous solutions, React. Polym. 23 (1994) 107–112.
[29] C.S. Sychov, M.M. Ilyin, V.A. Davankov, K.O. Sochilina, Elucidation of retention mechanisms on hypercrosslinked polystyrene used as column packing material for high-performance liquid chromatography, J. Chromatogr. A 1030 (2004) 17–24.
[30] C. Valderrama, J.L. Cortina, A. Farran, X. Gamisans, C. Lao, Kinetics of sorption of polyaromatic hydrocarbons onto granular activated carbon and Macronet hyper-cross-linked polymers (MN200), J. Colloid Interface Sci. 310 (2007) 35–46.
[31] R. Kunin, The use of macroreticular polymeric adsorbents for the treatment of waste effluents, Pure Appl. Chem. 46 (1976) 205–211.
[32] A.K. Nyhus, S. Hagen, A. Berge, Formation of the porous structure during the polymerization of *meta*-divinylbenzene and *para*-divinylbenzene with toluene and 2-ethylhexanoic acid (2-EHA) as porogens, J. Polym. Sci. Polym. Chem. 37 (1999) 3973–3990.
[33] M. Xu, Z. Shi, B. He, Oxidation of chloromethylated polystyrene during its Friedel–Crafts postcrosslinking, Ion Exch. Adsorpt. 12 (1996) 295–299 (in Chinese).
[34] G. Meng, A. Li, W. Yang, F. Liu, X. Yang, Q. Zhang, Mechanism of oxidative reaction in the post crosslinking of hypercrosslinked polymers, Eur. Polym. J. 43 (2007) 2732–2737.
[35] M. Streat, L.A. Sweetland, Removal of pesticides from water using hypercrosslinked polymer phases. Part 1. Physical and chemical characterization of adsorbents, Trans. IChemE B76 (1998) 115–126.
[36] B. Saha, M. Streat, Adsorption of trace heavy metals: application of surface complexation theory to a macroporous polymer and a weakly acidic ion-exchange resin, Ind. Eng. Chem. Res. 44 (2005) 8671–8681.
[37] T. Sano, M. Hasegawa, K. Kawakami, H. Yanagishita, Separation of methanol/methyl *tert*-butyl ether mixture by pervaporation using silicalite membrane, J. Membr. Sci. 107 (1995) 193–196.
[38] H.C. Trivedi, V.M. Patel, R.D. Patel, Adsorption of cellulose triacetate on calcium silicate, Eur. Polym. J. 9 (1973) 525–531.
[39] Y.S. Ho, G. McKay, Pseudo-second order model for sorption processes, Process Biochem. 34 (1999) 451–465.
[40] W.J. Weber, J.C. Morris, Adsorption Processes for Water Treatment, Butterworth, London, 1987.
[41] E. Guibal, C. Milot, J.M. Tobin, Metal-anion sorption by chitosan beads: equilibrium and kinetic studies, Ind. Eng. Chem. Res. 37 (1998) 1454–1463.
[42] M. Chabani, A. Amrane, A. Bensmaili, Kinetic modelling of the adsorption of nitrates by ion exchange resin, Chem. Eng. J. 125 (2006) 111–117.